since 1961

Baltica

BALTICA Volume 33 Number 2 December 2020: 128–145
https://doi.org/10.5200/baltica.2020.2.2

Palaeogene plutonic magmatism in Central Afghanistan, and its relation to the India-Eurasia collision

Gediminas Motuza, Saulius Šliaupa

Motuza, G., Šliaupa, S. 2020. Palaeogene plutonic magmatism in Central Afghanistan, and its relation to the India-Eurasia collision. *Baltica, 33 (2)*, 128–145. Vilnius. ISSN 0067-3064.
Manuscript submitted 2 February 2020 / Accepted 4 November 2020 / Published online 22 December 2020

Abstract. Numerous granitic intrusions occur along the southern margin of the Tajik Block and the Band-e-Bayan Zone in the Ghor Province of Central Afghanistan. Previously, they used to be linked to the Cimmerian igneous episodes of Triassic and Cretaceous ages. However, the new U-Pb dating has revealed that these granite intrusions occurred during the Eocene within a narrow time span of 41–36 Ma. They are related to the number of local depressions filled with the volcanic-sedimentary sequence of the same age. These data indicate an intense short-termed magmatic event that affected the region in the Palaeogene. The magmatism might be related to the India-Eurasia collision, which started approximately at the same time. It is likely to have induced the horizontal displacement of crustal blocks westwards along the Hari Rod fault.

Keywords*: Tadjik block; granite; isotopic dating; geochemistry; escape tectonics*

✉ *Gediminas Motuza (gediminas.motuza@gf.vu.lt), Institute of Geosciences, Vilnius University, M.K.Čiurlionio Str.21/27, LT-03101 Vilnius, Lithuania, Saulius Šliaupa (saulius.sliaupa@gamtc.lt), Nature Research Centre, Akademijos Str.2, LT-08412 Vilnius, Lithuania*

INTRODUCTION

The current paper presents results of the plutonic magmatism investigation performed in the Ghor Province in Central Afghanistan, its dating, and determination of its relation to the tectonic evolution. Numerous intrusions, mainly of granitic composition and, supposedly, of the Triassic, Jurassic, Cretaceous, Palaeogene or Neogene ages, were identified in the Ghor Province. They were related to various contemporaneous tectonic, mainly orogenic, events. However, less attention was paid to the consequences of the principal event in this region, i.e. the still ongoing India-Eurasia collision. The dating of this event as well as of its particular stages is still a debatable subject. Based on different proxies, various mechanisms of this collision and different time of its onset are suggested. In our paper, we present new data on the age of the magmatism that occurred along the Hari Rod fault system. The magmatism might have been triggered by the extrusion of crustal blocks along this and other fault systems, which are related to the India-Eurasia collision. A more accurate dating of the magmatism is expected to contribute to a better understanding of the history of this mega-tectonic event.

The current study is based on the field observations carried out by the authors along the Hari Rod River and its tributaries in 2008 and 2011, and on the subsequent petrological and geochemical studies (Fig. 1). The isotopic dating of samples from the representative intrusions was performed by Dr. Yury Amelin (Research School of Earth Sciences, Australian National University, Canberra). The study described in the current paper is a continuation of the research into the volcanic rocks contemporaneous with the intrusions distributed in the same area (Motuza, Šliaupa 2017b).

OVERVIEW OF PREVIOUS INVESTIGATIONS

The first systematic studies of plutonic magmatism in Afghanistan were carried out in the 1960s and 1970s as part of the geological mapping performed by teams of researchers from Germany, the USSR, France and other countries. The achieved study re-

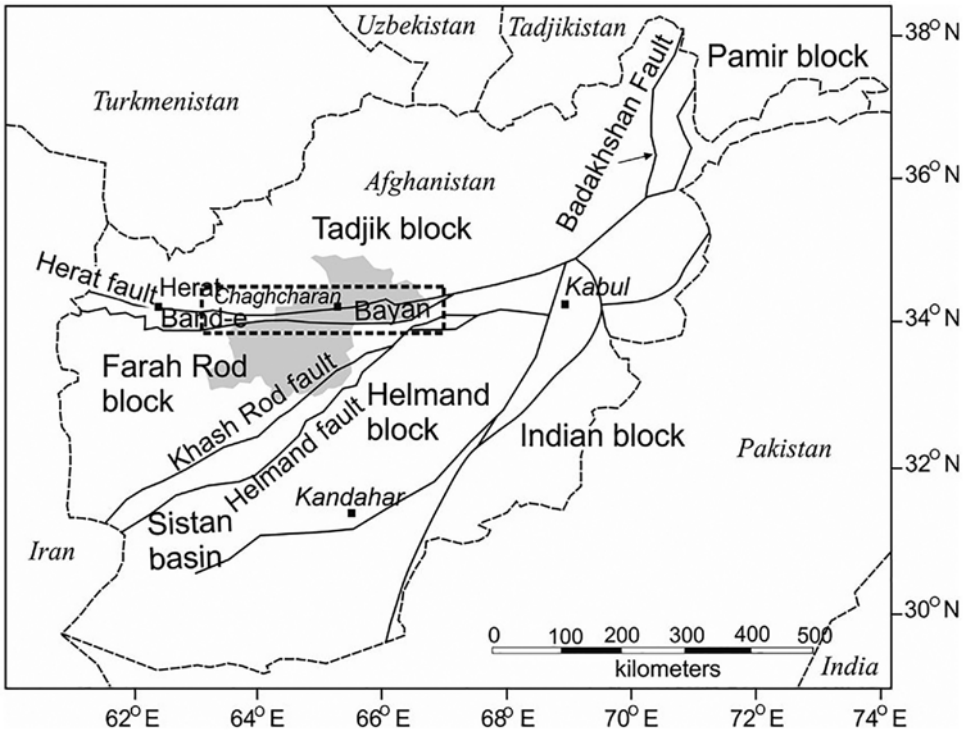

Fig. 1 Schematic tectonic map of Afghanistan (after Peters *et al*. 2007). The Ghor Province is indicated in grey, the field-work area is marked by a dashed line

sults included the compilation of geological maps and the accompanying monographs, presenting, *inter alia,* data and views on the history of magmatism. The most comprehensive early compilations were published by Wittekindt and Weppert (1973) on the geology of central and southern Afghanistan. In the explanatory notes to the map of the study area, Wittekindt (1973) presented dating results of 44 samples of intrusive rocks, which was performed employing Rb-Sr and K-Ar methods.

A comprehensive compilation of data on geological and mineral resources of Afghanistan was published by Abdullah and Chmyriov (1977, 1980, 2008), and Wolfart and Wittekindt (1980).

The first map of magmatic formations in Afghanistan, edited by Abdullah and Chmyriov (1977), summarised the work performed by Stazhilo-Alekseev *et al*. (1973). Eleven plutonic belts related to eight stages of intrusive magmatism, i.e. Precambrian, Early Carboniferous-Permian, Late Triassic, Early Cretaceous, Late Cretaceous-Paleocene, Eocene, Oligocene and Miocene have been mapped.

Since 1979 the main activities have been focused on the processing and analysis of archive information. Debon *et al*. (1987a,b and references therein) summarised the chemical analysis available, and results of K-Ar and Rb-Sr isotopic dating. They specified the age of plutonic magmatism in particular belts, and determined their affinity and geodynamic setting based on principles of the plate-tectonics theory. In Feroz Koh or Parapamisos, Band-e-Bayan, and Farah Rod Belts and those in adjacent areas, three stages of the intrusive magmatism of Triassic, Cretaceous, and Eocene-Oligocene ages were distinguished.

The most comprehensive compilation and reinterpretation of the existing geological materials was performed using remote sensing data by the United States Geological Survey (USGS) in co-operation with the Afghanistan Geological Survey. As a result, an updated geological map of Afghanistan supplemented with an extensive report was published (Doebrich, Wahl 2006; Peters *et al*. 2007). On this map, the Triassic, Cretaceous, Palaeogene, and Neogene granitic plutons were indicated in the Ghor Province.

A recently published review by Agemar Siehl (2015) has summarised 289 isotopic dates in Afghanistan. In plutonic belts of Feroz Koh and Band-e-Bayn in Central Afghanistan, Siehl (2015) distinguished several phases of granitic magmatism dating back to the Upper-Triassic-Lower Jurassic, Upper Jurassic-Late Cretaceous, Late-Upper Cretaceous, and the Tertiary ages. The author emphasised that the peak of the isotopic dates corresponds to the Palaeogene phase, which was related to the Himalayan orogeny, caused by the collision of Indian and Eurasian lithospheric plates. The preceding phases of magmatism were attributed to the Cimmerian orogeny, which was caused by the accretion of the continental blocks or terranes rifted from Gondwana, to Eurasia, thereby provoking the orogeny on the territory of the present-day Turkey, Iran, Afghanistan, and Tibet. This orogeny started in the Carboniferous, and continued until the Palaeogene

period. The ages of the rocks collected from the study area are summarised in Table 1 and Fig. 2. The recent isotopic U-Pb age estimates are scarce and are mainly available for the Kabul Block and Eastern Iran, particularly for the Lut Block and the Sistan Suture Zone (Suzuki 2002; Faryad *et al*. 2013; Bröcker *et al*. 2013; Faryad *et al*. 2016; Mohammadi *et al*. 2016).

Along with intrusive rocks of the study area, the volcanic lavas and pyroclastic rocks varying from basalt to andesite and dacite were studied (Abdullah, Chmyriov 2008; Motuza, Šliaupa 2017b). Volcanics are interbedded with sandstone, shale, and limestone, and are cut by minor subvolcanic diabase dykes and veins of quartz diorite, tonalite and granite. This sequence fills numerous grabentype structures (Fig. 2). According to characteristic fossils collected from the interbedded sedimentary layers, these volcanic rocks are attributed to the Palaeogene period (Abdullah, Chmyriov 2008).

GEOLOGICAL SETTING OF PLUTONIC ROCKS OF THE GHOR PROVINCE

One of the broadest overviews of the actual knowledge of the tectonic structure and evolution of crust in Afghanistan and in surrounding areas, throwing light on the broader context of the tectonic setting of the study area, and showing topics of ongoing debates, was provided by Agemar Siehl (2015). This area encompasses the southern part of the Tajik Block (also referred to as the North Afghanistan Block), the Band-e-Bayan Zone, and the northern part of the Farah Rod Block (Fig. 1). The southern marginal part of the Tajik Block is also often referred to as the Feroz Koh or the Parapamisos area (Debon *et al*. 1987a, b; Siehl 2015).

According to Siehl (2015 and references therein), the Tajik Block is a Variscan terrane of the Eurasian origin, while other authors (Abdullah, Chmyriov 1980; Kalvoda, Babek 2010; Peters *et al*. 2007) consider it to be a Proterozoic continental block derived from Gondwana and accreted to the Eurasian continent during the Carboniferous-Permian time.

The Band-e-Bayan Zone is a narrow W-E trending crustal block bounded by the large-scale Hari Rod fault (also referred to as the Herat fault) in the north. Siehl (2015) regards it as an exotic Gondwana-derived continental block accreted to the Tajik Block during the Permian-Triassic periods. Based on our data (Motuza, Šliaupa 2017a), the major lithologies of the Precambrian metamorphic supracrustal sequence, which is exposed in the southern margin of the Tajik Block and in the Band-e-Bayan Zone, form a common stratigraphic sequence, implying that the Band-e-Bayan Zone is a tectonized part of the Tajik continental block).

The Precambrian basement of the Band-e-Bayan Zone is covered by unmetamorphosed sedimentary and subordinate volcanic rocks ranging in age from the Ediacaran to the Neogene (Abdullah, Chmyriov 1980). The southern boundary of the Band-e-Bayan Zone with the Farah Rod Block is conditionally regarded to be the line limiting the distribution of the pre-Mesozoic rocks that are present in this zone but are not found in the Farah Rod Block.

The nature of the Farah Rod Block is not well understood. It is covered by an up to 12 kilometre thick sedimentary cover, as suggested by the magnetic field modelling (Wittekindt, Weppert 1973). Only the sediments of the Mesozoic and Cenozoic age are cropping out, while the presence of the Precambrian continental crust and the Palaeozoic sediments is not confirmed.

Table 1 Results of isotopic dating performed in Central Afghanistan

No.*	Locality	Method, mineral	Age, Ma	Reference
13 (24)	Southern Chaghcharan pluton	K-Ar, biotite	210; 213	Harre *et al.* in Wittekindt 1973
63	Northern Chaghcharan pluton	K-Ar, whole rock	194; 223	Zimmerman in Debon *et al*. 1987a
15	Obe pluton, NW part	K-Ar, whole rock	24; 21.3	Zimmerman in Debon *et al.* 1987a
		K-Ar, biotite	36.8	
		Rb-Sr, whole rock	35	Debon, Sonet 1982; Debon *et al.* 1987a
60	Obe pluton, SW part	K-Ar, whole rock	35.5; 39.7; 40; 47.7; 48.2	Zimmerman in Debon *et al*. 1987a
14 (21)	Cheste Sharif pluton	K-Ar, biotite K-Ar, muscovite	138; 94	Debon *et al*. 1987a
61	Cheste Sharif pluton	K-Ar, whole rock K-Ar, hornblende	247; 192.5; 399.6	Zimmerman in Debon *et al*. 1987a
		K-Ar, hornblende	400 ± 15	Debon *et al*. 1987a
62	Estern Cheste Sharif pluton	K-Ar, whole rock	43; 37	Zimmerman in Debon *et al*. 1987a
16 (22, 23)	Jam pluton	K-Ar, biotite K-Ar, muscovite	32.5; 33.2	Harre *et al*. in Wittekindt 1973
64	Kushnak pluton	K-Ar, whole rock	51; 69	Zimmerman in Debon *et al.* 1987a

*Numbers according to Debon *et al.* (1987a, b), in brackets – according to Wittekindt 1973.

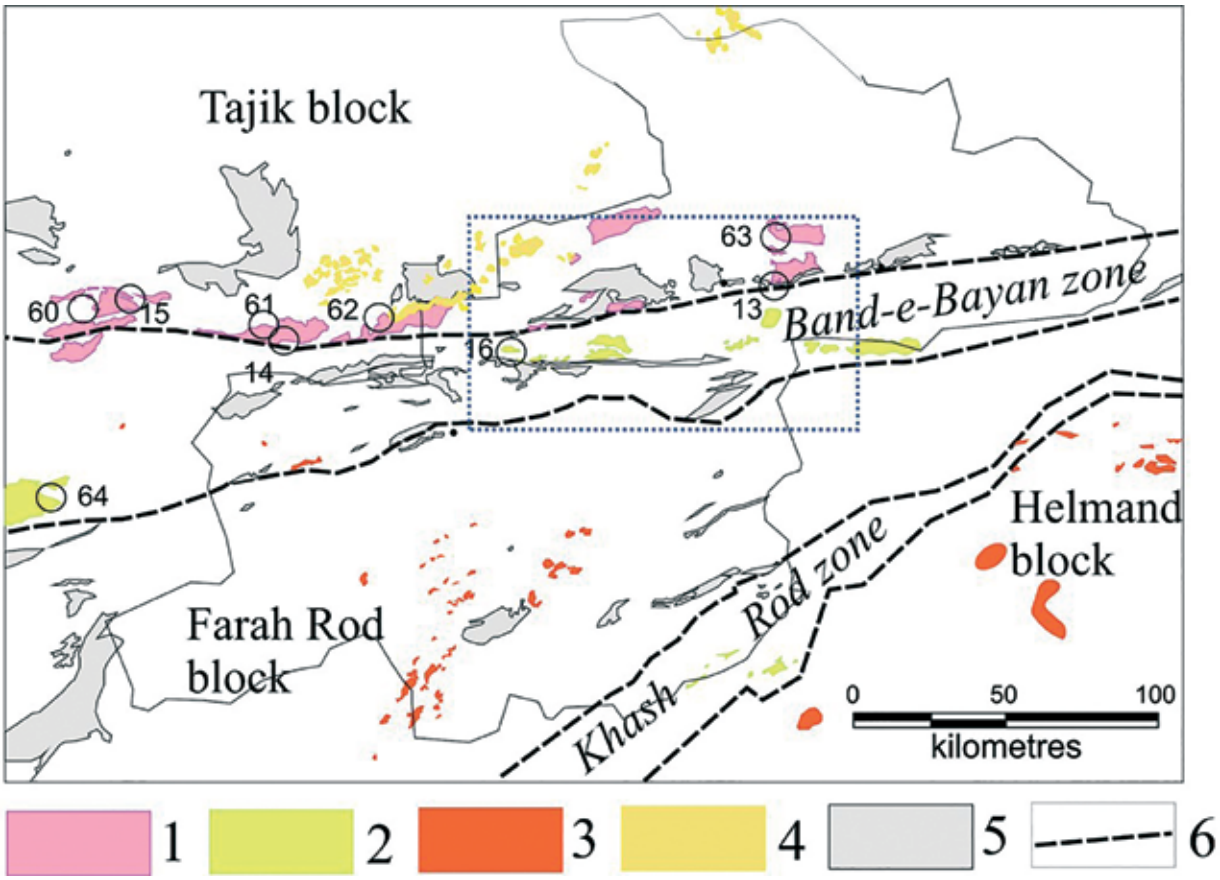

Fig. 2 Intrusive rocks of the Ghor Province (after Doebrich, Wahl 2006): 1 – Upper Triassic; 2 – Lower Cretaceous; 3 – Eocene; 4 – Miocene; 5 – areas of the Paleogene volcanic-sedimentary sequences; 6 – boundaries of major tectonic structures (after Peters *et al*. 2006). Numbered circles indicate the previously dated sites applying K-Ar and Rb-Sr methods (Table 1) (after Debon *et al*. 1987a). Boundaries of the province are marked by a black line. The area indicated in Fig. 3 is marked by a dashed line

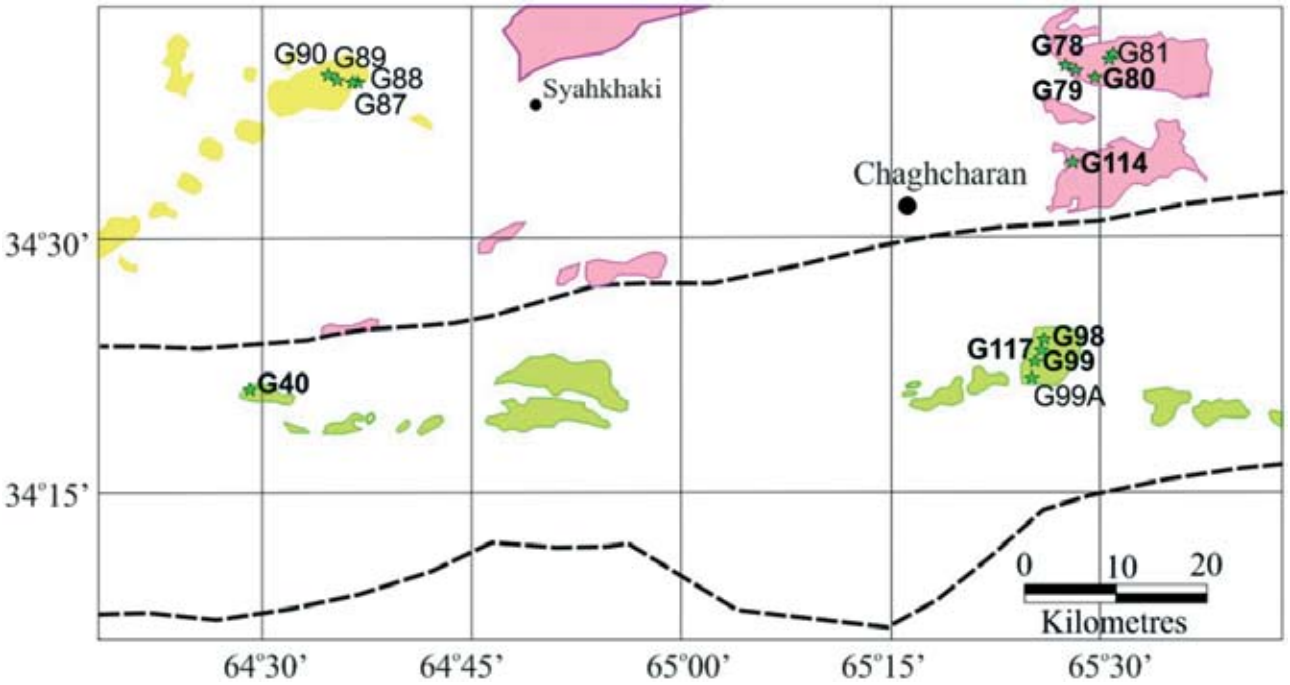

Fig. 3 Observation and sampling sites (green stars, numbered) of intrusive rocks in the Ghor Province. See Fig. 2 for symbols

PETROLOGY OF PLUTONIC ROCKS OF THE GHOR PROVINCE

Intrusions, marked as Triassic, Cretaceous, and Neogene on the map by Doebrich, Wahl (2006), were sampled during this study (Figs 2, 3).

Granodiorite intrusions, which in previous studies were attributed to the Triassic period, were investigated north-east of Chaghcharan (sites G78-81 and G114). These intrusions were previously considered to be covered by the Maastrichtian-Danian carbonate strata of the Upper Creatceous-Lower Palaeogene period. Meanwhile, we regard these intrusions as hosted by these sediments, and as cropping out in an erosional window (Figs 2; 4A).

Granodiorite is composed of (%): plagioclase – 35–40, microcline – 20–30, quartz – 20, biotite and hornblende – 15–20; accessory minerals – zircon, titanite, apatite, magnetite, tourmaline; secondary minerals – chlorite, muscovite, sericite, epidote.

The texture is porphyritic; phenocrysts of feldspar that are up to 10 mm in size are hosted by the medium-grained (1–5 mm) matrix. The rocks contain abundant decimetre-sized, lens-shaped or rounded enclaves of dark fine-grained rock. Some enclaves contain centimetre-sized feldspar phenocrysts similar to those of the host rocks (Fig. 4B), pointing to a magma mingling process. A sample of such an enclave, from site G114, is classified as biotite-hornblende quartz diorite, fine-grained, with phenocrysts of plagioclase 1–3 mm in size, often clearly zoned (Fig. 4C; Table 3, sample G114B).

Several intrusions, regarded as Cretaceous in age by previous researchers, are located in the Band-e-Bayan Zone. In the Jam area, situated in the western part of the Ghor Province, a number of small plutons were documented (G40). They are composed of light grey biotite granodiorite consisting of (%): plagioclase – 35, microcline – 30, quartz – 20, biotite – 15; accessory minerals - titanite, zircon, magnetite, apatite, tourmaline; secondary minerals: chlorite, sericite, muscovite, and epidote. The texture varies from coarse to medium-grained, with porphyry microcline phenocrysts up to 10 mm large. The structure is massive. The sampled pluton is hosted by the Carboniferous-Permian sedimentary and Proterozoic metamorphic rocks. A skarn body, composed of clinopyroxene partly substituted by actinolite, is located along the western contact of the intrusion with the hosting marble.

Another intrusion that was sampled during this study is also located in the Band-e-Bayan Zone, in the eastern part of the Ghor Province (sites G98, G117). It is not indicated on the map by Doebrich and Wahl (2006) and is presumably part of the intrusion located a few kilometres to the west (Fig. 3). The rock is classified as leucocratic K-feldspar granite (alaskite). It is yellowish white in colour, and is composed mainly of microcline and quartz, with subordinate plagioclase. There were no mafic minerals identified, except for rare chloritized biotite visible in hand specimens. Secondary minerals are represented by epidote, muscovite, and sericite formed at the expense of feldspars. The texture is porphyritic, formed by microcline phenocrysts up to 15–20 mm in size, often with granophyric intergrowths of quartz, in the groundmass of 5–10 mm sized grains. The structure is massive. Along the contact boundary with hosting Proterozoic schists, alaskite is transformed into the quartz muscovite rock, possibly during the initial stage of greisenization.

As stated by Doebrich and Wahl (2006), intrusions of the Neogene age form chains and clusters of small bodies in the Tajik Block in the western part of the Ghor Province, and in the adjacent Provinces of Herat and Badghis. They are composed of diorite, granodiorite, and syenite. No numerical age control is available to support the Neogene age of these intrusions. At the western margin of the Ghor Province, at the loc. G87–G90 (Fig. 3), we investigated a dioritic body, which had been considered by previous researchers to be of the Neogene age. We reclassified it as volcanic andesitic lava of the Eocene (54 Ma) based on Ar-Ar dating (Motuza, Šliaupa 2017b).

Fig. 4 Granodiorite from the Northern Chaghcharan pluton: A – exposure in an erosional window; outcrops of the roofing Cretaceous limestones are visible in the background. B – an enclave in the granodiorite with K-feldspar inclusions, indicating magma mingling (site G78), width of the picture ~30 cm); C – photomicrograph of the quartz diorite from the enclave (site G114B); crossed polars; width of the picture – 4.5 mm

ISOTOPIC DATING

Three intrusions were sampled for the isotopic dating: a granodiorite intrusion located in the Tajik Block (site G80), previously attributed to the Triassic; granodiorite (site G40) and alaskite (site G98) intrusions, both located in the Band-e-Bayan Zone and previously attributed to the Cretaceous (Doebrich, Wahl 2006).

The U-Pb dating of zircon was performed using SHRIMP RG and the techniques described by Tucker *et al.* (2011a, b). The data are presented in Table 2.

Sample G40 represents the biotite granodiorite intrusion located in the Jam area in the western part of the Ghor Province (coordinates: 34° 20'15"; 64° 28'56").

The zircon population consists of visually uniform, clear, elongated grains with relatively high cathodoluminescence (CL) brightness (Fig. 5). Most grains show a well-defined oscillatory zoned central part or the entire grain (domain 1), which in some cases (e.g., #2.2 and 10) is overgrown with structureless rims or tips (domain 2). Some grains (#4, 9, 11, and 15) contain relatively CL-bright cores with indistinct structures (domain 3). A few grains (#8, 13) contain CL-dark cores (domain 4).

Concentrations of U in zircons from domains 1–3 were found to range from 74 to 716 ppm, while those in zircons from domain 4 (dark cores) varied within the range of ca. 1200–1500 ppm. The concentration of Th/U is relatively high, varying between 0.43 and 1.23, and does not show systematic variations among the domains. Most grains are concordant and show uniform $^{238}U/^{206}Pb$ ages varying between 42 and 36 Ma, with a weighted average of 38.87 ± 0.95 Ma (2σ, MSWD = 1.06, n = 13), which can be interpreted as the age of magmatism (Fig. 6). A structurally distinct core and tip in grain #2 are of the same age.

Three grains (#7, 9 and 15) are older and are strongly positively discordant (Fig. 6C). The minimum age of these inherited grains is indicated by the dates of their $^{238}U/^{206}Pb$, which vary between 46 and 228 Ma. The maximum age is derived from two-point discordia lines for each of these grains and the age of the rock, which is 38.87 Ma. This calculation suggests that these zircons did not experience Pb loss before getting entrained into magma at ca. 39 Ma.

Sample G80 is a hornblende-biotite granodiorite (coordinates: 34° 39'20"; 65° 29'37"). Two populations of zircon are present in this sample: clear colourless prismatic and pale-brown short-prismatic (Fig. 7). CL patterns match the visual appearance: clear long grains show bright CL with complex linear or oscillatory zoning (domain 1), short-prismatic grains have medium intensity CL with similar patterns (domain 2). Some short-prismatic grains (e.g. #12 and 13) contain CL-dark, structureless rims, but these rims are too narrow to place the primary beam.

In long-prismatic CL-bright grains, U concentrations were found to vary between 184 and 947 ppm, and the Th/U ratio was found to be relatively uniform varying between 0.54 and 0.79. One grain (#5, the youngest in the population) was found to have an unusually low Th/U ratio of 0.10. The weighted average of $^{238}U/^{206}Pb$ ages for this population is 36.35 ± 0.93 Ma (2σ), which is interpreted as the age of the rock (Fig. 8A, B). One grain (#1) of the long-prismatic, clear population has an unusually high U concentration of 1430 ppm, and the Th/U ratio of 1.06, which is higher than that in other grains. It is also slightly older, with the age estimated at 42.0 ± 3.4 Ma (2σ). The origin of this grain is unclear. It might be inherited from earlier intrusion phases of the same age as represented here by alaskite (sample G98).

The concentrations of U in the second group of grains represented by short-prismatic ones range between 274 and 728 ppm, and the Th/U ratio varies within the range of 0.38–0.69. Six out of eight analyses of seven grains of the short-prismatic population show uniform $^{238}U/^{206}Pb$ ages in the range 212–196 Ma, with a weighted average of 203.9 ± 6.3 Ma. (Fig. 8C, D).

This can be interpreted as the age of a xenocryst in igneous protolith, or in detrital zircon from sedimentary rocks that melted at ca. 36 Ma. One grain of similar appearance (#8) is older, with the age estimated at 305 Ma. The short-prismatic grain #13 contains a CL-bright structureless inner core, surrounded by a CL-medium outer core, and then by a CL-dark rim. The concentration of U in its inner core is unusually low (64 ppm), and its apparent $^{238}U/^{206}Pb$ age, which is estimated at 639 Ma, is unusually old, but this date is unreliable due to the high content of non-radiogenic Pb.

These data suggest that this granodiorite crystallized in the Eocene from the melt that was derived from an igneous source of the latest Triassic-Jurassic age or younger sedimentary rocks, or was contaminated by these lithologies. This interpretation is consistent with field observations showing that these intrusions are hosted by the Upper Cretaceous-Palaeogene carbonates, and are cropping out in erosional windows (Fig. 4A), as our observations show.

Sample G98 was collected from an alaskite body (coordinates: 34° 23'57"; 65° 26'00"), which marks the eastern end of the chain of granitic intrusions in the Band-e-Bayan Zone.

The rock contains short prismatic zircon grains of variable quality (Fig. 9). Most grains are characterized by medium-dark to bright CL, and oscillatory, banded or complex curved zoning or their combination (domain 1). Some of these grains are overgrown by darker rims (domain 2). A few grains have similar zoning patterns but much brighter CL (domain 3).

The U concentrations vary from ca. 100 to 800 ppm, and Th/U ratios from 0.13 to 1.22. These values are

Table 2 U-Pb SHRIMP data for zircons in granitic rocks in the Ghor Province

Spot Name	Struct. domain	U, ppm	Th, ppm	^{206}Pb, ppm	^{207}Pb /^{206}Pb	% err	^{208}Pb /^{206}Pb	% err	Total ^{208}Pb /^{232}Th	% err
G40-1	1	239	140	1.2	0.045	5.5	0.189	6.5	0.0018	107
G40-2.1	1	572	348	2.9	0.048	3.4	0.202	3.9	0.0019	38
G40-2.2	2	233	130	1.2	0.049	5.2	0.200	6.2	0.0021	22
G40-3	1	85	102	0.4	0.048	9.8	0.381	8.6	0.0019	0
G40-4	3	155	108	0.8	0.044	10.2	0.221	8.8	0.0019	60
G40-5	1	124	146	0.6	0.052	6.6	0.408	5.8	0.0021	26
G40-6	1	88	58	0.5	0.040	11.1	0.229	11.3	0.0022	0
G40-7	1	538	588	3.3	0.478	1.4	21.214	0.9	0.1358	80
G40-8	4	1526	789	8.2	0.047	1.5	0.176	1.3	0.0021	43
G40-9	3	97	54	3.0	0.294	1.7	23.338	1.0	1.4666	96
G40-10	2	716	361	3.8	0.242	37.9	10.502	33.3	0.1245	96
G40-11	3	133	90	0.7	0.051	7.5	0.227	6.6	0.0020	73
G40-12	1	111	77	0.6	0.034	22.2	0.189	24.1	0.0017	53
G40-13	4	1256	526	6.7	0.048	2.0	0.139	3.3	0.0020	0
G40-14	1	74	78	0.4	0.048	8.4	0.344	7.5	0.0021	80
G40-15	3	155	94	3.1	0.352	1.5	22.624	0.9	0.8388	268
G80-1	1	1429	1468	8.1	0.048	2.8	0.399	1.6	0.0025	20
G80-2.1	1	398	229	2.0	0.049	3.7	0.191	4.4	0.0019	53
G80-2.2	1	359	245	1.7	0.049	4.2	0.243	6.9	0.0019	30
G80-3	2	655	242	17.4	0.050	1.3	0.118	2.0	0.0095	54
G80-4	1	184	141	1.0	0.049	5.5	0.256	5.9	0.0020	53
G80-5	1	396	38	1.8	0.048	6.7	0.039	17.3	0.0021	47
G80-6.1	1	947	650	4.8	0.049	2.5	0.236	3.0	0.0020	37
G80-6.2	1	554	405	2.8	0.049	3.2	0.247	3.5	0.0019	89
G80-6.3	1	307	161	1.5	0.049	4.2	0.187	5.2	0.0020	18
G80-7	2	393	263	10.8	0.050	1.6	0.225	2.0	0.0105	146
G80-8	2	649	267	27.1	0.057	1.0	0.121	1.5	0.0138	52
G80-9	1	623	439	3.1	0.049	3.1	0.231	3.5	0.0018	26
G80-10	1	398	294	1.9	0.043	4.4	0.232	4.5	0.0017	2
G80-11	1	343	211	1.7	0.050	4.0	0.196	5.2	0.0018	33
G80-12	2	662	277	19.1	0.051	1.2	0.132	2.3	0.0103	54
G80-13	3	64	45	8.4	0.277	3.0	0.794	3.3	0.1685	5
G80-14	2	728	303	20.5	0.051	1.2	0.135	1.7	0.0103	37
G80-15.1	2	274	105	8.3	0.090	2.7	0.222	2.2	0.0196	11
G80-15.2	2	688	276	18.7	0.064	1.5	0.167	1.7	0.0128	21
G98-1	1	187	113	13.4	0.066	1.2	0.212	1.6	0.0285	22
G98-2	1	287	86	20.7	0.058	1.0	0.097	1.9	0.0261	40
G98-3	1	387	238	26.8	0.059	0.9	0.213	1.9	0.0270	32
G98-4	1	829	101	58.6	0.076	3.1	0.088	7.9	0.0570	15
G98-5	1	493	79	34.0	0.058	1.2	0.053	2.1	0.0255	52
G98-6	1	778	494	6.8	0.047	2.0	0.209	2.3	0.0032	53
G98-7	1	104	64	13.0	0.081	1.2	0.230	1.6	0.0525	22
G98-8	3	258	186	1.4	0.048	4.6	0.254	4.9	0.0022	47
G98-9	3	122	144	0.7	0.055	6.0	0.419	5.4	0.0023	0
G98-10	3	140	75	0.7	0.051	8.4	0.191	7.0	0.0021	72
G98-11	1	576	108	41.1	0.060	0.7	0.070	1.6	0.0299	27
G98-12.1	2	805	248	52.6	0.077	1.0	0.148	1.9	0.0353	10
G98-12.2	1	363	175	33.1	0.086	1.7	0.224	1.5	0.0479	9
G98-13	1	377	147	27.5	0.058	0.9	0.128	1.4	0.0271	69
G98-14	1	493	292	32.1	0.057	1.0	0.189	1.5	0.0234	30
G98-15	1	791	158	57.7	0.057	0.6	0.064	1.4	0.0263	32
G98-16	1	792	270	57.9	0.058	1.0	0.109	1.2	0.0264	39
G98-17	1	127	73	11.6	0.063	1.8	0.183	2.0	0.0328	31

Table 2 (continued)

Spot Name	Struct. domain	Total $^{238}U/^{206}Pb$	% err	Total $^{207}Pb/_{206}Pb$	% err	204corr $^{206}Pb/^{238}U$ Age	1σ err	207corr $^{206}Pb/^{238}U$ Age	1σ err	208corr $^{206}Pb/^{238}U$ Age	1σ err
G40-1	1	170.20	4.2	0.0454	5.5	37.3	1.6	37.8	1.6	37.8	1.8
G40-2.1	1	171.18	4.0	0.0482	3.4	36.9	1.5	37.5	1.5	37.5	1.7
G40-2.2	2	168.63	4.4	0.0487	5.2	37.4	1.6	38.0	1.7	37.8	1.8
G40-3	1	163.00	4.9	0.0481	9.8	39.4	1.9	39.4	1.9	39.7	2.5
G40-4	3	157.47	4.5	0.0438	10.2	39.3	2.0	41.0	1.8	41.0	2.1
G40-5	1	164.14	4.4	0.0521	6.6	36.0	1.8	38.9	1.7	38.6	2.2
G40-6	1	151.29	4.9	0.0402	11.1	42.5	2.1	42.8	2.1	42.2	2.4
G40-7	1	138.20	4.3	0.4782	1.4	46.3	2.0	21.1	3.4	-550.1	80.7
G40-8	4	160.68	4.0	0.0470	1.5	39.7	1.6	40.0	1.6	39.9	1.7
G40-9	3	27.72	4.0	0.2941	1.7	228.0	9.0	158.2	11.1	-3460.7	593.9
G40-10	2	161.80	4.0	0.2419	37.9	39.6	1.6	29.9	4.9	-179.7	79.7
G40-11	3	159.26	4.3	0.0510	7.5	39.7	1.8	40.1	1.7	40.3	2.0
G40-12	1	159.13	4.4	0.0343	22.2	38.1	2.1	41.0	1.9	41.3	2.3
G40-13	4	160.76	3.9	0.0482	2.0	40.0	1.6	39.9	1.6	40.0	1.7
G40-14	1	148.87	4.5	0.0477	8.4	42.0	2.1	43.1	2.0	43.2	2.5
G40-15	3	43.08	4.0	0.3524	1.5	147.7	5.9	91.2	8.2	-1930.2	289.3
G80-1	1	152.30	4.0	0.0477	2.8	42.0	1.7	42.1	1.7	40.7	2.1
G80-2.1	1	169.73	4.0	0.0493	3.7	37.3	1.5	37.7	1.5	37.8	1.7
G80-2.2	1	178.95	4.1	0.0491	4.2	34.8	1.5	35.8	1.5	35.6	1.7
G80-3	2	32.40	3.9	0.0499	1.3	195.7	7.6	196.0	7.6	196.2	8.1
G80-4	1	166.08	4.2	0.0492	5.5	38.1	1.6	38.6	1.6	38.6	1.9
G80-5	1	189.80	4.3	0.0476	6.7	33.3	1.5	33.8	1.5	33.8	1.5
G80-6.1	1	170.04	4.1	0.0492	2.5	37.7	1.5	37.7	1.5	37.6	1.7
G80-6.2	1	169.80	4.0	0.0493	3.2	37.7	1.5	37.7	1.5	37.7	1.7
G80-6.3	1	176.75	4.1	0.0492	4.2	35.5	1.5	36.3	1.5	36.1	1.6
G80-7	2	31.13	3.9	0.0501	1.6	203.6	7.9	203.9	7.9	203.1	8.9
G80-8	2	20.59	3.9	0.0574	1.0	305.4	11.7	303.8	11.7	307.6	12.5
G80-9	1	174.00	4.0	0.0486	3.1	36.6	1.5	36.9	1.5	37.0	1.7
G80-10	1	178.56	4.1	0.0425	4.4	36.4	1.5	36.2	1.5	36.2	1.7
G80-11	1	172.24	4.1	0.0495	4.0	36.7	1.5	37.2	1.5	37.4	1.7
G80-12	2	29.85	3.9	0.0505	1.2	212.3	8.2	212.4	8.2	212.9	8.8
G80-13	3	6.60	4.0	0.2771	3.0	639.2	32.2	669.5	42.8	640.2	53.4
G80-14	2	30.45	3.9	0.0507	1.2	208.1	8.0	208.2	8.1	208.4	8.6
G80-15.1	2	28.44	3.9	0.0904	2.7	207.6	8.3	211.6	8.4	211.9	9.4
G80-15.2	2	31.63	3.9	0.0638	1.5	198.1	7.7	197.2	7.7	196.9	8.3
G98-1	1	11.98	3.9	0.0655	1.2	511.1	19.4	511.9	19.7	511.9	21.7
G98-2	1	11.93	3.9	0.0581	1.0	518.1	19.5	518.7	19.9	518.8	20.5
G98-3	1	12.42	3.9	0.0590	0.9	497.9	18.8	498.0	19.1	495.0	20.9
G98-4	1	12.15	3.9	0.0765	3.1	497.0	18.8	497.5	19.1	498.0	19.7
G98-5	1	12.45	3.9	0.0575	1.2	497.6	18.9	497.7	19.2	497.6	19.4
G98-6	1	98.44	4.0	0.0466	2.0	65.3	2.6	65.2	2.6	65.1	2.9
G98-7	1	6.86	4.0	0.0811	1.2	868.0	32.9	862.8	33.9	861.4	36.8
G98-8	3	153.25	4.1	0.0485	4.6	41.6	1.7	41.8	1.7	41.5	2.0
G98-9	3	151.56	4.6	0.0553	6.0	42.4	1.9	41.9	1.9	41.6	2.5
G98-10	3	165.39	4.2	0.0512	8.4	39.5	1.7	38.6	1.6	38.6	1.8
G98-11	1	12.04	3.9	0.0605	0.7	512.3	19.3	512.3	19.6	511.8	19.9
G98-12.1	2	13.15	3.9	0.0767	1.0	459.9	17.4	460.7	17.7	461.3	18.8
G98-12.2	1	9.42	3.9	0.0862	1.7	630.3	23.6	629.9	24.2	627.1	26.5
G98-13	1	11.77	3.9	0.0578	0.9	525.8	19.9	525.7	20.3	524.7	21.2
G98-14	1	13.19	3.9	0.0569	1.0	471.0	17.8	471.0	18.1	471.7	19.7
G98-15	1	11.78	3.9	0.0574	0.6	524.9	19.9	525.5	20.2	525.2	20.5
G98-16	1	11.76	4.0	0.0579	1.0	525.7	20.1	526.3	20.4	526.3	21.2
G98-17	1	9.46	4.0	0.0628	1.8	646.5	24.3	646.8	24.9	647.6	26.8

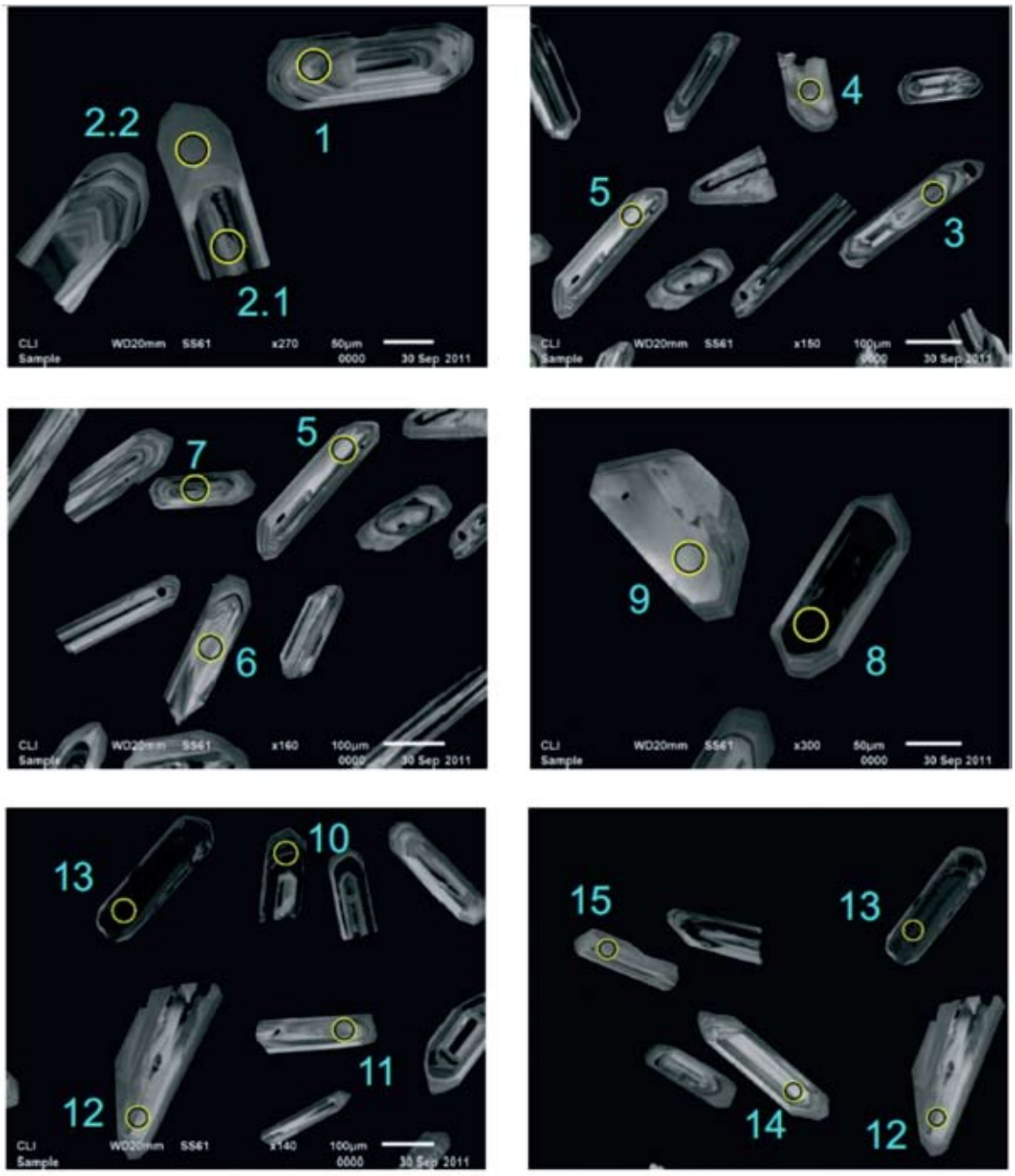

Fig. 5 Cathodoluminescence images of dated zircon grains from granodiorite, site G40. The circles mark the analyzed domains commented in the text

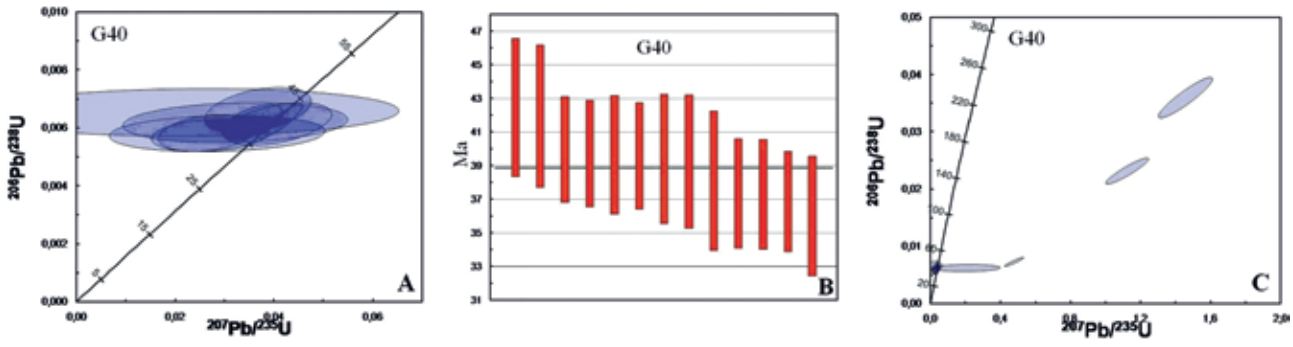

Fig. 6 Dating of the granodiorite sample G40: A, B – concordia and mean age calculation diagrams for the youngest zircons; C – diagram for older discordant inherited grains

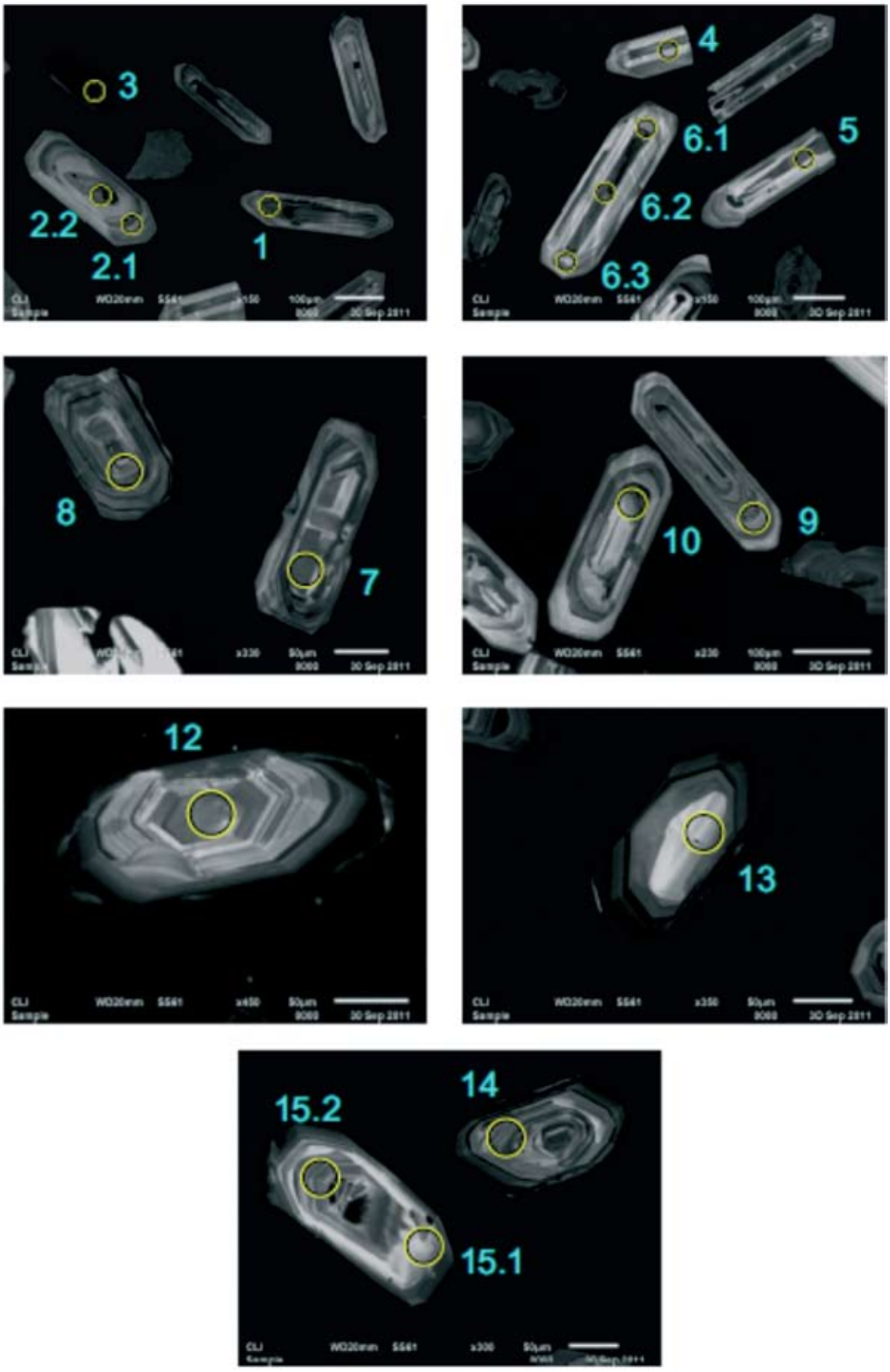

Fig. 7 Cathodoluminescence images of dated zircon grains from the granodiorite sample G80. The circles mark the analyzed domains commented in the text

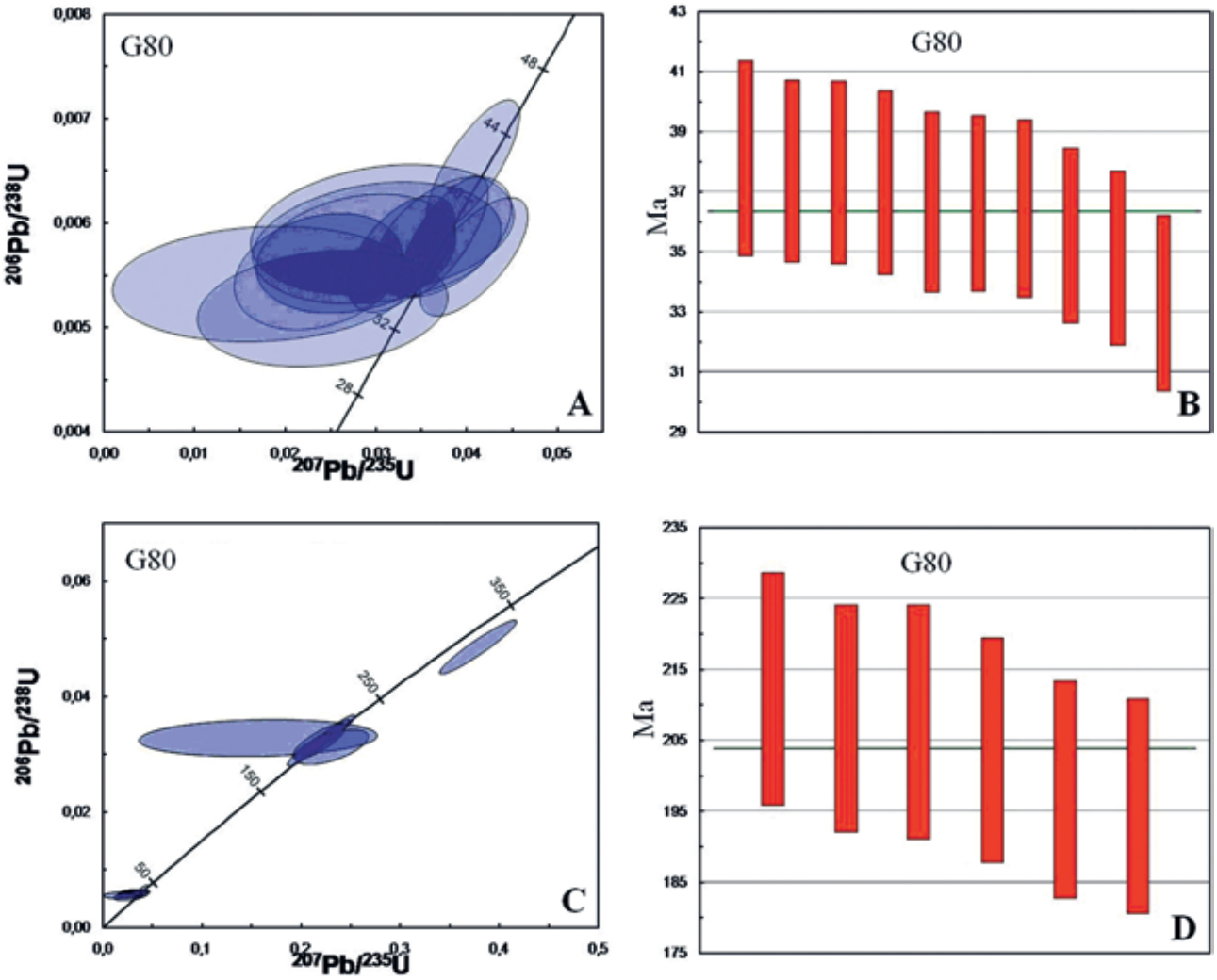

Fig. 8 Concordia and mean age calculation diagrams for zircons from the granodiorite sample G80. A, B – youngest zircons; C, D – inherited zircon population

consistent with the igneous origin of zircons.

The U-Pb systems in all the grains examined are concordant or nearly concordant. Three grains with very bright CL (domain 3) have consistent $^{238}U/^{206}Pb$ ages with the weighted average of 41 ± 2 Ma (Fig. 10).

Ten analyses of grains belonging to domain 1 yielded consistent $^{238}U/^{206}Pb$ ages between 526 and 471 Ma, with a weighted average of 507 ± 12 Ma (2σ) (Fig. 10). Two grains and one core (#12.2) were found to be older with $^{238}U/^{206}Pb$ ages varying between 630 and 868 Ma. These grains have lower U values and brighter CL than the majority of the population. The intergrowth of dark CL (domain 2) with high-U (805 ppm) in the core aged 630 Ma is slightly younger than the main part of the core, and its $^{238}U/^{206}Pb$ age is 460 Ma.

The interpretation we offer is that this rock was formed at 41 Ma (Eocene, Lutetian) by remelting and extensive assimilation of 507 Ma Cambrian igneous rocks or sediments containing some older material. This is indicated by inherited cores of 507 Ma with yet older material.

GEOCHEMISTRY OF PLUTONIC ROCKS OF THE GHOR PROVINCE

Four intrusions were sampled and seven chemical analyses were carried out for the geochemical characterisation of intrusive rocks (Fig. 3; Table 3). Two of them were previously regarded as Late Triassic, and the other two as Early Cretaceous. The andesitic lava, previously regarded as Neogene diorite, was described by Motuza, Šliaupa (2017b).

The analyses were performed in AcmeLabs, Canada. The abundance of major oxides and trace elements including REE were determined by ICP-MS following a lithium metaborate/tetraborate fusion and nitric acid digestion of a 0.2 g sample.

Samples that were not altered by weathering, hydrothermal or other secondary processes were selected for analysis. The absence of secondary processes was confirmed by low LOI ranging from 0.8 to 2.7%.

The investigated rocks are slightly peraluminous, subalkaline, and are attributed to calc-alkaline series.

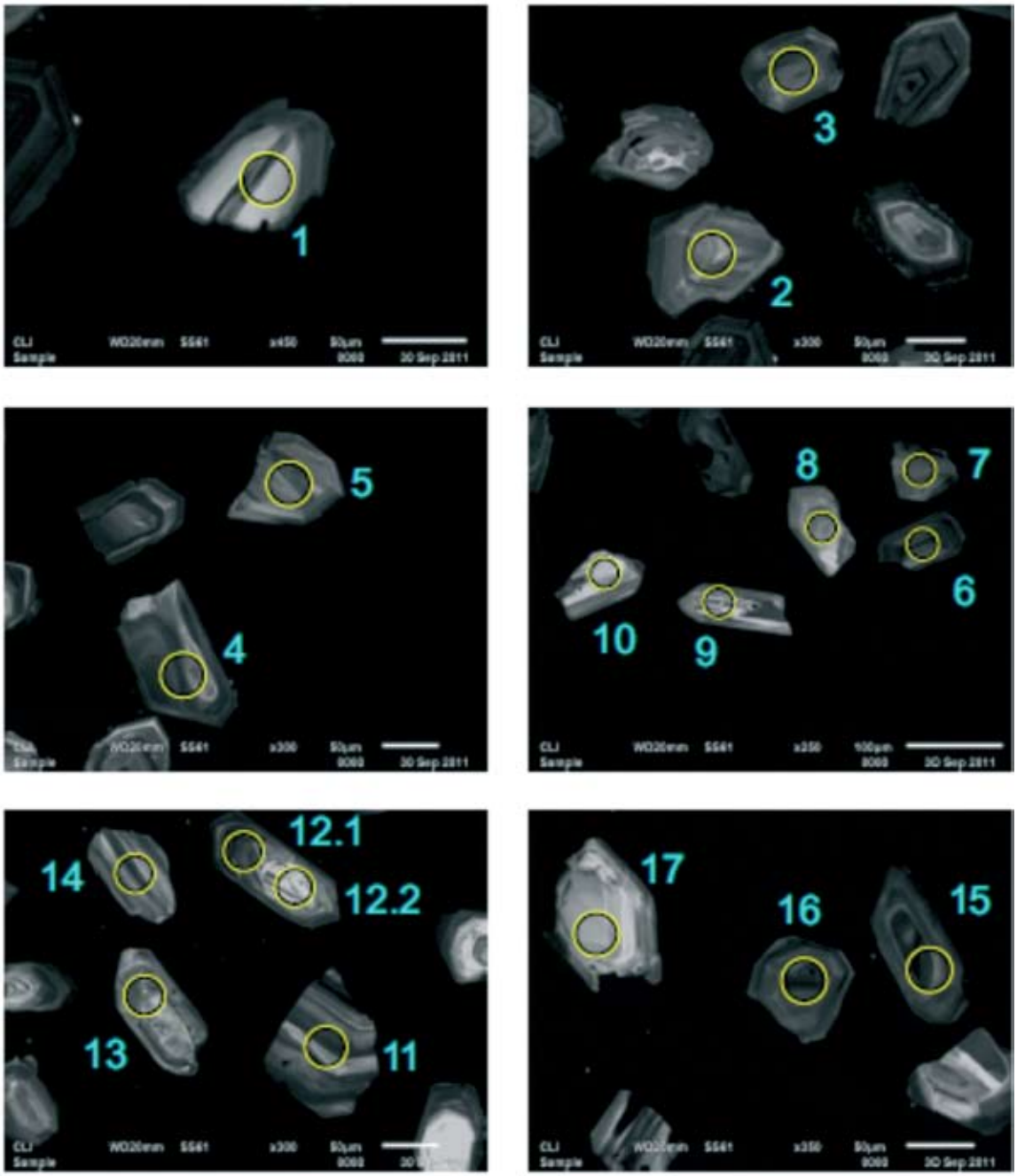

Fig. 9 Cathodoluminescence images of dated zircon grains from the alaskite sample G98. The circles mark the analyzed domains commented in the text

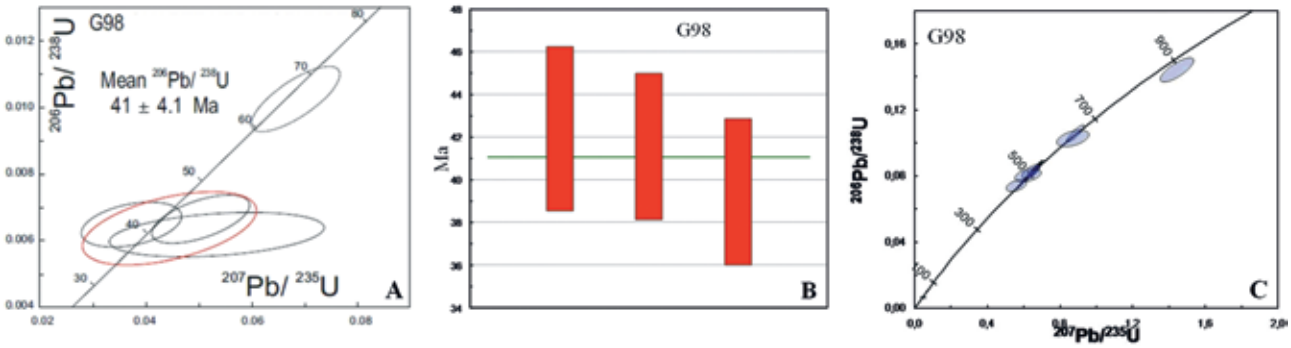

Fig. 10 Concordia (A) and mean age calculation diagrams (B) for the youngest zircons and the concordia diagram for inherited zircons (C) from the alaskite sample 98

Table 3 Chemical composition of granitic rocks of the Ghor province (major oxides in %, trace elements in ppm)

Sample	G40	G78	G80	G114B	G98	98-1	G117
Lithology	Granodiorite	Granodiorite	Granodiorite	Diorite*	Alaskite	Alaskite	Alaskite
SiO_2	65.23	68.15	68.17	60.51	75.42	76.07	72.66
TiO_2	0.71	0.4	0.41	0.60	0.08	0.07	0.21
Al_2O_3	15.64	15.09	14.66	16.24	12.26	11.89	15.45
FeO_{tot}	4.11	3.95	3.94	5.82	0.87	1.12	1.73
MnO	0.05	0.09	0.09	0.12	0.01	0.02	0.03
MgO	1.43	1.47	1.74	2.57	0.16	0.15	0.64
CaO	3.13	3.49	3.48	5.71	0.13	0.21	0.10
Na_2O	4.07	3.61	3.07	3.44	0.16	0.18	1.46
K_2O	3.63	2.61	3.27	1.96	9.34	8.89	5.42
P_2O_5	0.26	0.12	0.12	0.15	0.04	0.03	0.04
Cr_2O_3	0.004	0.005	0.005	0.004	0.004	0.002	<0.002
LOI	1.4	0.8	0.8	2.7	1.4	1.3	2.2
Sc	9	9	10	13	3	3	5
V	61	78	85	109	<8	<8	10
Co	51.8	60.1	69	12.1	72.1	0.9	1.5
Ni	7.9	4.1	6.2	4.2	1.8	1.8	1.9
Cu	12	6.1	10.2	18.8	12.2	5.1	6.2
Zn	36	33	43	62	13	11	19
Ga	18.7	14.7	15.2	17.9	16.6	16.2	19.9
Rb	105.5	94.4	115	97.9	424.4	405.9	250.3
Sr	507.8	291.5	309.6	327.8	32.8	40.3	49.2
Y	23.6	22	18.2	19.3	65.2	50	42.0
Zr	285.5	152.3	129.9	127.9	79.9	79.9	126.6
Nb	28.5	10.4	9.2	8.5	10.5	8.8	15.1
Cs	1.8	3.2	6.8	5.3	8.8	8	7.0
Ba	972	411	525	446	310	401	480
La	72.5	30.9	33.5	15.6	14.1	12.8	37.2
Ce	131	56.5	61.5	33.9	33.3	29.2	78.5
Pr	14.82	6.41	6.64	4.29	4.23	3.66	8.98
Nd	51.1	22.1	22.9	17.0	14.1	11.7	30.8
Sm	7.58	4.03	3.63	3.78	3.55	3.09	6.74
Eu	1.63	0.79	0.79	0.98	0.11	0.1	0.33
Gd	5.79	3.7	3.26	3.50	4.94	3.88	6.07
Tb	0.87	0.52	0.42	0.56	1.04	0.82	1.10
Dy	4.52	3.35	2.7	3.26	9.3	6.92	6.65
Ho	0.82	0.73	0.62	0.62	1.99	1.53	1.30
Er	2.4	2.03	1.6	1.86	6.65	5.11	4.03
Tm	0.35	0.34	0.3	0.28	1.11	0.83	0.66
Yb	2.21	2.27	1.93	1.87	7.5	5.92	4.44
Lu	0.3	0.37	0.32	0.27	1.05	0.84	0.64
Hf	7.3	5	4.1	3.7	3.2	3.8	4.3
Ta	1.7	0.9	1.3	0.7	2.4	2.1	1.7
Pb	2.6	2.1	3.3	7.7	45.3	25.9	17.5
Th	19.7	12.4	20.8	6.3	18.9	16.7	24.6
U	3	2.8	5.8	1.6	5	3.7	3.0
W	366.5	415.9	506	<0.5	570.6	6.1	4.2
Mo	0.2	0.2	0.2	0.6	0.5	0.7	0.4
Be	2	1	2	2	2	3	5
As	0.9	0.7	1.6		4	2.7	
Cd	<0.1	<0.1	<0.1	2.2	<0.1	<0.1	21.3
Au	<0.5	<0.5	<0.5	0.7	<0.5	<0.5	0.7
TOT/C	0.11	0.02	0.34	0.32	0.02	<0.02	0.02
TOT/S	0.02	<0.02	<0.02	<0.02	<0.02	<0.02	<0.02

*Inclusion in granodiorite presumably formed by magma mingling.

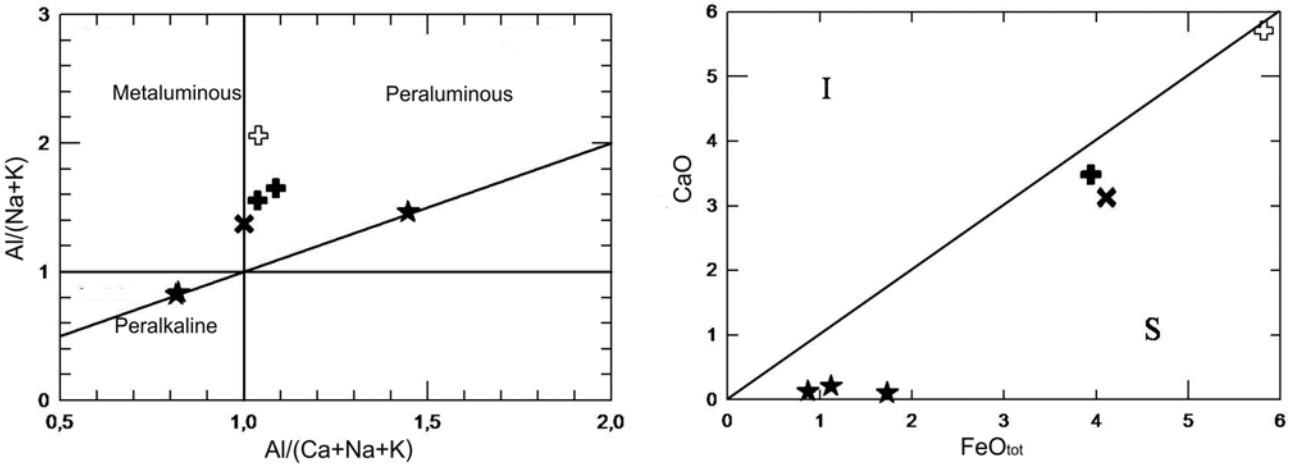

Fig. 11 Shand's index (after Maniar, Piccoli 1989), and CaO vs. FeO_{tot} diagrams for granitic rocks of the Ghor Province. I, S – fields of I-, and S-type granites (after Chappell, White 2001). Symbols: ✚ – granodiorite (samples G78, G80); ✜ – inclusion in granodiorite (sample G114B); ★ – alaskite (samples G98; G98-1; G117); ✖ – granodiorite (sample G40)

Some of them are classified as high-K rocks. Specific patterns reveal alaskite, which is metaluminous, peralkaline, enriched in potassium (K_2O up to 8.89%).

By the criteria developed by Chappell, White (2001) (Fig. 11), the rocks correspond to S-type granite in spite of the fact that their compositions differ. Alaskite rocks do not contain mafic minerals, and CaO and FeO contents in them are very low. On the contrary, the contents of these components in quartz diorite enclave from granodiorite (Sample 114B) are much higher than in other sampled rocks. On the discrimination diagram by Whalen *et al.* (1977), all points cluster in I&S-type granite field (Fig. 12).

By the criteria set by Frost *et al.* (2001), the investigated rocks are classified as magnesian, calc-alkalic and alkali-calcic granites typical of the subduction-related continental magmatic arcs and bear affinity to the granitic plutons of the Cordilleras of North America as a reference representative of this group (Fig. 13).

On the tectonic setting diagrams, the points cluster in the volcanic arc and collisional granites fields (Fig. 14).

On the REE abundance diagram, the studied rocks are slightly enriched in LREE with a minor negative Eu anomaly, while alaskite reveals a prominent negative Eu anomaly explained by the predominant K-feldspar content with respect to plagioclase (Fig. 15).

Our results show that the geochemical patterns of the investigated plutonic rocks are variable. These rocks were probably formed by melting of the Earth's crust of different composition, with admixture of mantle-derived basalt magma in various proportions. The crustal source is suggested by the peraluminous character of the examined rocks and the presence of inherited zircons of different ages. The abundant coeval basalt lava flows observed in the same area and intermediate composition enclaves in granodiorites (Fig. 4) suggest the hybridisation with basic magma (Motuza, Šliaupa 2017b). There is also a distinction

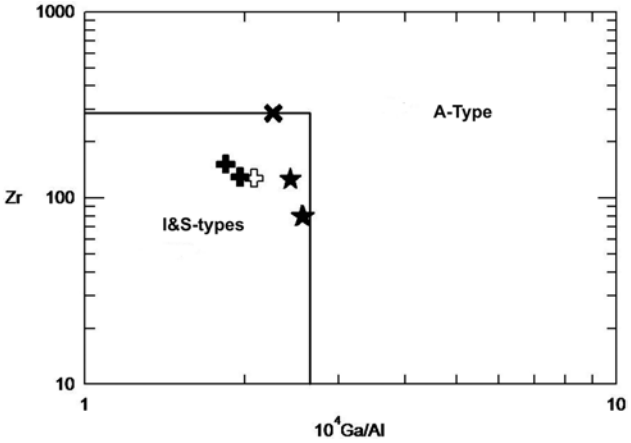

Fig. 12 Zr vs. Ga/Al diagram for granitic rocks of the Ghor Province (after Whalen *et al*. 1977). See Fig. 11 for symbols

between T_{Zr} sensu (Harrison, Watson 1983) in alaskite (G98 = 743 °C), and granodiorite (G40 = 816 °C) samples, which might be explained by fluid enrichment of alaskitic magma, which lowers the temperature of its crystallisation. Tectonic setting discrimination criteria for intrusions indicate an active continental margin, collisional or continental volcanic arcs setting, with no intraplate tectonic setting signatures.

DISCUSSION

The newly acquired U-Pb dates do not support the Triassic and Cretaceous ages of intrusions in Central Afghanistan, which are indicated on the geological map by Doebrich, Wahl (2006) (Figs 2, 3).

The intrusions located in the Band-e-Bayan Zone are shown as Cretaceous on the map, while our dating results indicate the Palaeogene age. The K-Ar data (Table 1) also point to the Palaeogene age, except a single measurement from the Khushnak pluton that corresponds to the Late Cretaceous.

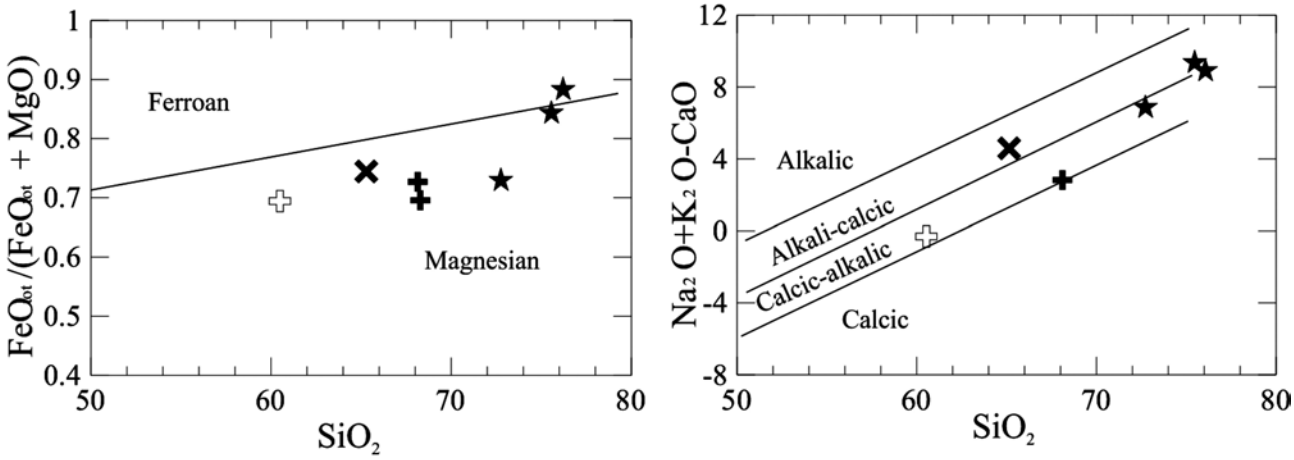

Fig. 13 $FeO_{tot}/(FeO_{tot} + MgO)$ *vs*. SiO_2 and $Na_2O + K_2O$ - CaO *vs*. SiO_2 classification diagrams (after Frost *et al*. 2001) for granitic rocks of the Ghor Province. See Fig. 11 for symbols

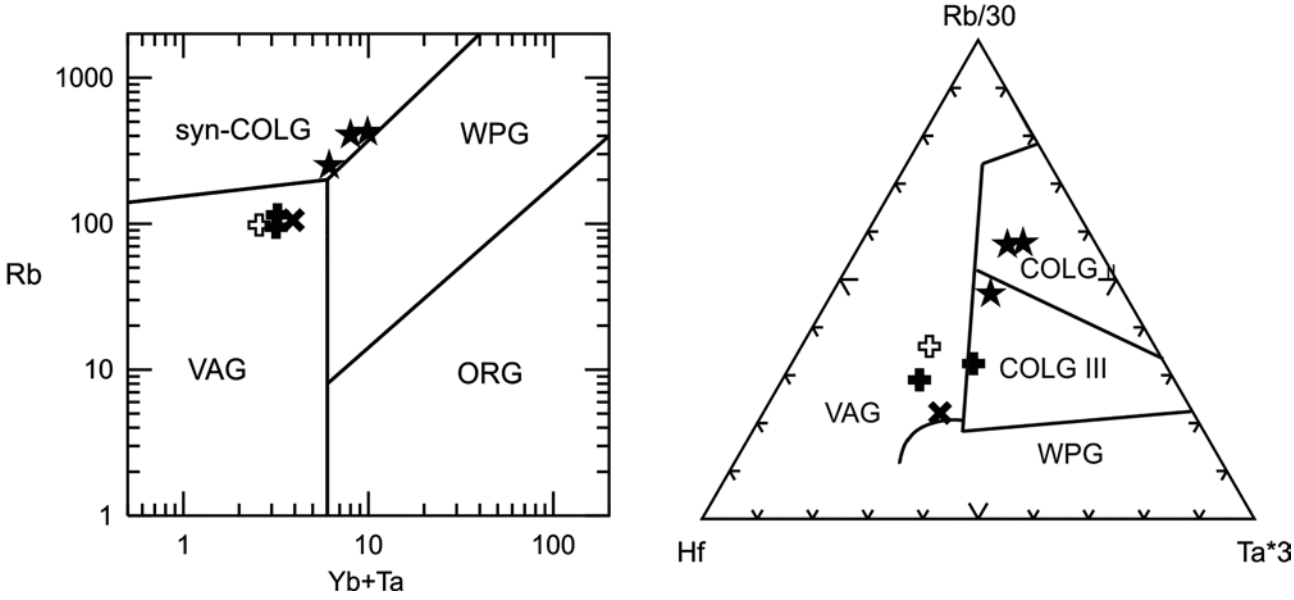

Fig. 14 Tectonic setting discrimination diagrams for intrusive rocks of the Ghor Province: Rb *vs*. Yb + Ta (Pearce *et al*. 1984) and Hf-Rb/30-Ta*3 (Harris *et al*. 1986). WPG – within-plate granites; VAG – volcanic arc granites; COLG II – syn-collisional leucogranites; COLG III – late or post-collisional calc-alkaline granites. See Fig. 11 for symbols

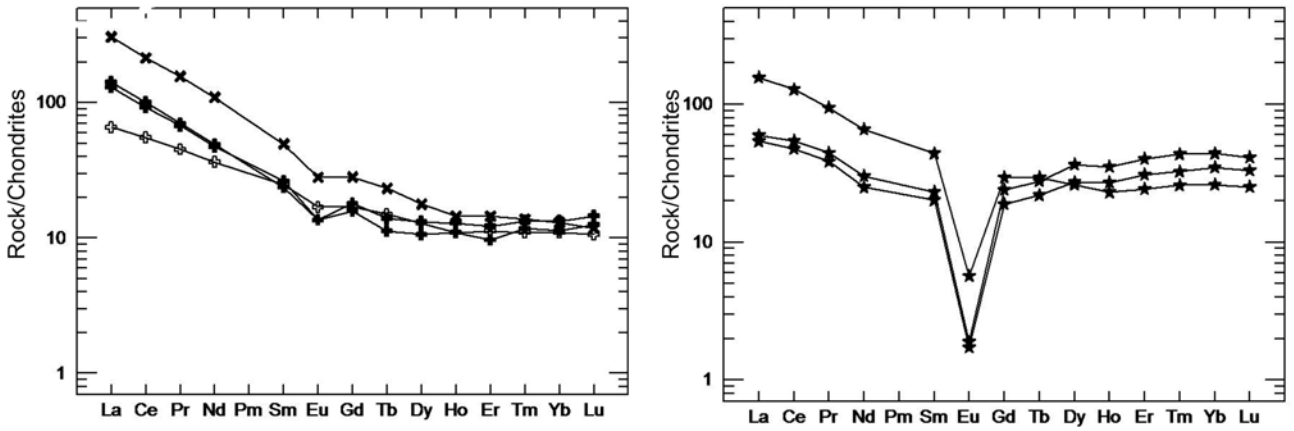

Fig. 15 Chondrite normalized REE abundance diagram for granodiorite (left) and alaskite (right) of the Ghor Province. See Fig. 11 for symbols

All the intrusions situated along the southern margin of the Tajik Block are shown as Triassic on the map. Neogene intrusions are indicated in the westernmost part of the Ghor Province. The dating of Obe pluton using K-Ar and Rb-Sr methods revealed Palaeogene and Neogene ages (35–37; 21.3–24 Ma); the analysis of the Cheshte Sharif pluton shows a wide range of dates including the Early Devonian, Triassic, Jurassic, Cretaceous, and the Palaeogene age. The Chaghcharan pluton was previously dated back to the Triassic age (210 and 212 Ma), while results of our dating performed using the U-Pb method show that crystallisation of this pluton occurred in the Palaeogene (36.35 ± .93 Ma). A similar disagreement was found to exist about the age of the intrusion in the belt located close to Bamyan (east of the Ghor Province), which was previously presumed to be Triassic, whereas the findings of U-Pb dating revealed the Permo-Carboniferous age 298 ± 28 Ma (Suzuki *et al.* 2002).

In summary, the data on the age of intrusions in the Feroz Koh and Band-e-Bayan magmatic belts obtained applying K-Ar and U-Pb methods indicate that the predominant age of these intrusions is the Palaeogene. However, a few of the obtained K-Ar results contradict those of the U-Pb dating.

The new isotopic age determinations have raised doubts about the existence of separate Feroz Koh and Band-e-Bayan plutonic belts dating back to the Triassic and Cretaceous ages and hence, an extensive Palaeogene magmatic phase has been hypothesized.

The older, inherited zircon grains detected in the samples analysed provide additional information on the history of the plutonic magmatism.

The oldest grains encountered in the alaskite sample (G98) are dated as 868 Ma and 630 Ma, which corresponds to the Tonian and Ediacaran periods of the Neoproterozoic era. This intrusion is hosted by a sequence of metamorphic rocks composed of felsic gneisses (metapsammites), greenschists (basic metavolcanics), and marbles (Motuza, Šliaupa 2017a). On the map by Doebrich, Wahl (2006), the age of the sequence is indicated as Mesoproterozoic but this age has not been confirmed by isotopic dating. The relic zircon grains found in the Palaeogene alaskite intrusion were probably derived from the hosting metapsammites. The age of these grains indicates the possible lower age limit of the metamorphic sequence. In some places, the basement is covered by unmetamorphosed sediments of the late Neoproterozoic era. These data suggest the Ediacaran age of the metamorphic basement in the Band-e-Bayan Zone and possibly in the southern margin of the Tajik Block.

Another group of relic zircon grains date from the Cambrian and Ordovician ages (526–471 Ma; 460 Ma). The source of these zircons is difficult to identify, because plutonic rocks of the Cambrian and Ordovician ages are not exposed on the territory of Afghanistan. The provenance of detrital zircons of this age might be Gondwana, from which the Tajik Block and Band-e-Bayan Zone were derived, as suggested by Motuza, Šliaupa (2017a).

Carboniferous (350 Ma) zircons are present in the same sample (G78). The evidence of carboniferous magmatic activity was documented in the study area. The Carboniferous age of rhyolitic tuffs was estimated based on the interbedding of paleontologically dated sedimentary rocks recognised in the marginal part of the Tajik Block in the westernmost part of the Ghor Province (Doeberich, Wahl 2006). The Carboniferous (298 ± 28 Ma) intrusion, which was dated applying the U-Pb method, is located close to Bamyan, east of the study area (Suzuki *et al.* 2002).

Triassic relict zircon grains were detected in samples from the Jam and Chaghcharan intrusions (G40; G80). The Jam intrusion is hosted by the Carboniferous-Permian sedimentary and Proterozoic metamorphic sequences. The Chaghcharan intrusion spatially associates with Cretaceous-Palaeogene limestones. Triassic rocks are not known in these areas. By origin, these grains can possibly be related to the Triassic intrusions remelted during the Palaeogene. Triassic volcanic rocks are widely distributed throughout the North Afghanistan Block, which could have been associated with intrusive magmatism.

The rock ages estimated in this study indicate an intensive phase of magmatism, both of plutonic, subvolcanic, and volcanic types, along the southern margin of the Tajik Block and in the Band-e-Bayan Zone during the Palaeogene period (mainly Eocene), and call into question the previous dating of plutonic rocks in Central Afghanistan back to Triassic, Cretaceous, and Neogene ages.

The geochemical characteristics of magmatic rocks, i.e. S-type affinity, magnesian, calc-alkalic and alkali-calcic types, are similar to those of subduction-related or active continental margin granites. On the tectonic setting diagrams (Fig. 14), granodiorites cluster in the field of volcanic arc granites, while alaskites are confined to the field of syn-collisional granites.

Nevertheless, it is difficult to reconcile the model of collisional subduction-related magmatism with the regional tectono-stratigraphic setting. The Palaeogene magmatic phase was predated by the carbonate platform sedimentation in the Upper Cretaceous-Lower Palaeogene (Maastrichtian-Danian) implying little or no tectonic activity. It was only in the narrow zone along the southern edge of the Tajik Block and in the Bande-e-Bayan Zone that these sedimentary strata as well as the Palaeogene volcanic-sedimentary succession were deformed in the Neogene. It is suggested that granitic magma was generated by the melting

of the old crust formed in the subduction-zone or in the continent-continent collision environment (Eby 1992). Assimilation of the crustal material is indicated by the occurrence of older zircons, as discussed above. Enclaves of quartz diorite, abundant in granodiorites, suggest mingling of melts. A similar conclusion was reached by Pang *et al*. (2013) who had been investigating the Palaeogene magmatism of eastern Iran, which postdated subduction events there, despite geochemical evidence for the collisional tectonic setting.

The Palaeogene magmatism of the Ghor Province is coeval with the onset of the India-Eurasia collision that started in the Eocene. The more likely time as evaluated by different researchers based on various proxies is different, but fits into the time interval 55–34 Ma (Aitchison *et al*. 2007; Seton *et al*. 2010; Najman *et al.* 2010). This collision might have caused intracontinental shortening, tectonic extrusion, and lateral movements of particular blocks along the strike-slip fault systems (Tapponier *et al.* 1981; Debon *et al*. 1987a, b; Siehl 2015). The triangle-shaped Farah Rod Block was displaced along the border with the Tajik Block (including the Band-e-Bayan Zone), which caused a tectonic extension, triggering plutonic and volcanic magmatism (Treloar, Izatt 1993; Motuza, Šliaupa 2017b).

CONCLUSIONS

The U-Pb dating of zircons using the SHRIMP technique evidences intense igneous activity along the southern margin of the Tajik Block and the Band-e-Bayan Zone over a brief time span 41 ± 2 – 36.35 ± 0.95 Ma, corresponding to the Eocene Epoch.

Intrusive rocks display the geochemical features of subduction and collisional granitoids; however, no evidence of coeval subduction and collisional processes has been currently discovered in the region.

Inheritance of the geochemical features of the previous events is alternatively suggested for the Palaeogene intrusions.

Magmatism is likely to have been triggered by the India-Eurasia collision, resulting in escape (extrusive) tectonic movements along the southern margin of the Tajik Block.

ACKNOWLEDGMENTS

The study was financed by the Development Cooperation and Democracy Promotion Program coordinated by the Ministry of Foreign Affairs of the Republic of Lithuania. We are especially thankful to the Lithuanian Provincial Reconstruction Team (PRT) in the Ghor Province for the excellent organisation of the field work. The contribution of Prof. Dr. Agemar Siehl (University of Bonn) (sharing of important materials and participation in discussions) is acknowledged and highly appreciated. The authors express gratitude to Dr. Yury Amelin (Research School of Earth Sciences, Australian National University, Canberra), for dating the samples, and to Dr. Robert Tucker (US Geological Survey) for intermediation for rock dating. Many thanks go to reviewers Dr. Ewa Krzemińska and Dr. Randell Stephenson for valuable remarks and suggestions.

REFERENCES

Abdullah, S.H., Chmyriov, V.M. 1977. *Geological map of Afghanistan*, *Annex 1 to Geology and Mineral Resources of Afghanistan*. Book I, Geology, Moscow, Nedra, scale 1:2,500,000 [In Russian].

Abdullah, S.H., Chmyriov, V.M. 1980. *Geology and Mineral Resources of Afghanistan*, Book I, Geology, Moscow, Nedra, 535 pp. [In Russian].

Abdullah, S., Chmyriov, V.M. (eds.). 2008. *Geology and Mineral Resources of Afghanistan*. *British Geological Survey Occasional Publication*, 2 Volumes, 15.

Aitchison, J.C., Ali, J.R., Davis, A.M. 2007. When and where did India and Asia collide? *Journal of Geophysical Research: Solid Earth 112*, B05423, doi:10.1029/2006JB004706.

Bröcker, M., Rad, F.G., Burgess, R., Theunissen, S., Paderin, I., Rodionov, N., Salimi, Z. 2013. New age constraints for the geodynamic evolution of the Sistan Suture Zone, eastern Iran. *Lithos 170–171*, 17–34.

Chappell, B.W., White, J.R. 2001. Two Contrasting Granite Types: 25 years later. *Australian Journal of Earth Sciences 48*, 489–499.

Debon, F., Sonet, J. 1982. Typologie chimique et chronologie comparées des granitoïdes de l'Hindou Kuch – Badakhshan occidental et du Feroz Koh (Afghanistan). *9ème Réun. ann. Sci. Terre, 184*, Soc. géol. Fr. édit.

Debon, F., Afzali, H., Le Fort, P., Sonet, J., Zimmermann, J.L. 1987a. Plutonic rocks and associations in Afghanistan: typology, age and geodynamic setting. *Sciences De La Terre. Memoires 49*, 132.

Debon, F., Afzali, H., Le Fort, P., Sonet, J. 1987b. Major intrusive stages in Afghanistan: typology, age and geodynamic setting. *Geologishe Rundschau 76/1*, 245–264.

Doebrich, J.L., Wahl, R.R. 2006. Geological and Mineral Resource Map of Afghanistan. *U.S. Geological* Survey *Open-File Report* 2006–1038, scale 1:850,000, http://pubs.usgs.gov/of/2006/1038/.

Eby, G.N. 1992. Chemical subdivision of the A-type granitoids: Petrogenetic and tectonic implications. *Geology 20*, 641–644.

Faryad, S.W., Collett, S., Petterson, M., Sergeev, S.A. 2013. Magmatism and metamorphism linked to the accretion of continental blocks south of the Hindu Kush, Afghanistan. *Lithos 175–176,* 302–314, DOI 10.1016/j.lithos.2013.04.016.

Faryad, S.W., Collett, S., Finger, F., Sergeev, S., Čopjako-

va, R., Siman, P. 2016. The Kabul Block (Afghanistan), a segment of the Columbia Supercontinent, with a Neoproterozoic metamorphic overprint. Gondwana Research 34, 221–240.

Frost, B.R., Barnes, C.G., Collins, W.J., Arculus, R.J., Ellis, D.J., Frost, C.D. 2001. A Geochemical Classification for Granitic Rocks. *Journal of Petrology 42*, *11*, 2033–2048.

Harris, N.B.W., Pearce, J.A., Tindle, A.G. 1986. Geochemical characteristics of collision-zone magmatism. In: Coward, M.P., Ries, A.C. (eds), *Collision Tectonics*. *Geological Society of London Special Publication 19*, 67–81.

Harrisson, T.M., Watson, A.B. 1983. Zircon saturation revisited: temperature and composition effects in a variety of crustal magma types. *Earth and Planetary Science Letters, vol. 64 (2)*, 295–304. https://doi.org/10.1016/0012-821X(83)90211-X.

Kalvoda, J., Bábek, O. 2010. The Margins of Laurussia in Central and Southeast Europe and Southwest Asia. *Gondwana Research 17*, 526–545.

Maniar, P.D., Piccoli, P.M. 1989. Tectonic discrimination of granitoids. *Geological Society of America Bulletin 101*, 635–643.

Mohammadi, A., Burg, J-P., Bouilhol, P., Ruh, J. 2016. U–Pb geochronology and geochemistry of Zahedan and Shah Kuh plutons, southeast Iran: Implication for closure of the South Sistan suture zone. *Lithos* 248–251, 293–308.

Motuza G., Šliaupa, S. 2017a. Supracrustal suite of the Precambrian crystalline crust in the Ghor Province of Central Afghanistan. *Geoscience Frontiers 8*, *1*, 125–135, DOI: 10.1016/j.gsf.2015.12.011.

Motuza, G., Šliaupa, S. 2017b. Paleogene volcanism in Central Afghanistan: Possible far-field effect of the India-Eurasia collision. *Journal of Asian Earth Sciences 147*, 502–515.

Najman, Y., Appel, E., Boudagher-Fadel, M., Bown, P., Carter, A., Garzanti, E., Godin, L., Han, J., Liebke, U., Oliver, G., Parrish, R., Vezzoli, G. 2010. Timing of India-Asia collision: Geological, biostratigraphic, and palaeomagnetic constraints. *Journal of Geophysical Research 115*, B12416.

Pang, K.-N., Chung, S.-L., Zarrinkoub, M.H, Khatib, M.M., Mohammadi, S.S., Chiu, H.Y., Chu, Ch.-H., Lee, H.-Y., Lo, Ch.-H. 2013. Eocene–Oligocene post-collisional magmatism in the Lut–Sistan region, eastern Iran: Magma genesis and tectonic implications. *Lithos* 180–181, 234–251.

Pearce, J.A., Harris, B.W., Tindle, A.G. 1984. Trace element discrimination diagrams for the tectonic interpretation of granitic rocks. *Journal of Petrology 25*, 956–983.

Peters, S.G., Ludington, S.D., Orris, G.J., Sutphin, D.M., Bliss, J.D., Rytuba, J.J. (eds.), and the U.S. Geological Survey-Afghanistan Ministry of Mines Joint Mineral Resource Assessment team. 2007. Preliminary Non-Fuel Mineral Resource Assessment of Afghanistan. *U.S. Geological Survey Open-File Report 2007–1214*.

Seton, M.M., Müller, R.D., Zahirovic, S., Gaina, C., Torsvik, T., Shephard, G., Talsma, A., Gurnis, M., Turner, M., Maus, S., Chandler, M. 2012. Global continental and ocean basin reconstructions since 200 Ma. *Earth-Science Reviews 113*, 212–270.

Siehl, A. 2015. Structural setting and evolution of the Afghan orogenic segment – a review. In: Brunet, M.-F., McCann, T., Sobel, E.R. (eds). Geological Evolution of Central Asian Basins and the Western Tien Shan Range. *Geological Society, London, Special Publications 427*, http://doi.org/10.1144/SP427.8.

Stazhilo-Alekseev, K.F., Chmyriov, V.M., Mirzad, S.H., Dronov, V.I., Kafarskiy, A.K. 1973. The main features of magmatism of Afghanistan. *Geology and mineral resources of Afghanistan*, 31–43. Geological Survey of Afghanistan.

Suzuki, K.S., Yutaka, N., Dunkley, D., Mamoru, A. 2002. Significance of c. 300 Ma CHIME zircon age for post-tectonic granite from the Hercynian suture zone, Bamian, Afghanistan. *Bulletin of Nagoya University Museum 18*, 67–73.

Tapponnier, P., Mattauer, M., Proust, F., Cassaigneau, C. 1981. Mesozoic ophiolites, sutures, and large-scale tectonic movements in Afghanistan. *Earth and Planetary Science Lettres 52*, 355–371.

Treloar, P.J., Izatt, C.N. 1993. Tectonics of the Himalayan collision between Indian Plate and the Afghan Block: a synthesis. In: Treloar, P.J., Searle, M.P. (eds), *Himalayan Tectonics: Geological Society, London, Special Publications 74*, 69–87.

Tucker, R.D., Roig, J.Y., Macey, P.H., Delor, C., Amelin, Y., Armstrong, R.A., Rabarimanana, M.H., Ralison, A.V. 2011a. A new geological framework for south-central Madagascar, and its relevance to the "out-of-Africa" hypothesis. *Precambrian Research 185*, 109–130.

Tucker, R.D., Roig, J.Y., Delor, C., Amelin, Y., Gonsalves, P., Rabarimanana, M.H., Ralison, A.V., Belcher, R.V. 2011b. Neoproterozoic extension in the Greater Dharwar Craton: a reevaluation of the ''Betsimisaraka suture'' in Madagascar. *Canadian Journal of Earth Sciences 48,* 389–417.

Whalen, J.B., Currie, K.L., Chappell, B.W. 1977. A-type Granites: Geochemical Characteristics, Discrimination and Petrogenesis. *Contributions to Mineralogy and Petrology 95*, 407–419.

Wittekindt, H. 1973. *Erläuterung zur Geologischen Karte von Zentral- und Süd-Afghanistan 1:500 000*. Hannover, Bundesanstalt fur Bodenforshung.

Wittekindt, H., Weppert, D. 1973. Geological map of central and southern Afghanistan: German Geological Mission to Afghanistan. *Geological Survey of the Federal Republic of Germany*, scale 1:500,000.

Wolfart, R., Wittekindt, H. 1980. Geologie von Afghanistan. *Beiträge zur Regionalen Geologie der Erde 14*, 500 pp.